

The investigation of high-cycle loading from the perspective of seismology

R. Kliukas, M.K. Leonavičius, G. Petraitis & R. Stonkus

Vilnius Gediminas Technical University, Lithuania



SUMMARY:

High-cycle loading, making a part of a broad spectrum of vibrations and seismic loads, may be considered separately, when the number of cycles reaches 10^9 . The stresses developed under such loading are below the ultimate strength. In designing various building constructions, as well as mining equipment, and planning their long service life, pulsating loads should be evaluated in addition to commonly applied loads. Long-term effect of these loads on the particular elements of metal structures is similar to the phenomenon of metal fatigue, developing due to variable loading. The paper presents the results obtained in the experimental analytical research, aimed at evaluating strength of materials under high-cycle loading. Specimens' resistance to crack propagation was tested, based on the specified and extended methods. The limit stress intensity factors and the relationships between the crack growth rate and stress intensity factor are determined. The analysis of crack formation and propagation in the flaw area based on the use of the scanning electron microscope (SEM) is performed. The effect of non-uniform zones on crack development is also determined. The results obtained may be used for calculating strength and durability of structures subjected to high-cycle loading as well as for determining their safety factors.

Keywords: crack, high-cycle fatigue, stress intensity factor

1. INTRODUCTION

Now, the calculation of the ability of structural elements to withstand cyclic loading ($> 10^8$) is based on the limit strength, determined, when the number of cycles $N = 10^6 \dots 10^7$. When the number of cycles is larger, the interpolated strength is used in calculation methodologies. This is not always justified because, with the increase of the number of cycles ($> 10^7$), the fracture mechanism changes. In addition, the cases of overloading may occur. Seismic loads, acting in various directions, are also of the cyclic nature.

Complex strength evaluation of the main structures of buildings, located in the areas of high seismicity, may be performed by carrying out the experimental research and testing natural and semi-natural specimens, thereby improving the calculations methods.

2. TESTING PROCEDURES

The standard eccentric tension (CT) specimens and special semi-natural steel specimens, cut out of a real structure, were tested. Only high-quality specimens, i.e. those, having no defects according to the results of inspection by non-destructive methods, were used for high-cycle loading tests. Their quality was checked by non-destructive (optic, ultrasonic and luminescent-magnetic) methods. The welded joint, the surrounding area and the whole tested part of the element, i.e. the main surface of the metal plate, were inspected. CT specimens and the specimen of rectangular cross-section (27x60 mm), with the welded joint in the middle of the tested part, were cut out of the same welded plate.

The chemical composition of the base metal: C 0.05-0.06%, Mn 0.82-0.85, Cr 0.10-0.12, Ni 0.20-0.22, Si 0.27-0.29, Mo 0.05-0.54, Cu 0.032-0.034 and weld metal: C 0.03-0.04%, Mn 1.20-1.25, Cr 0.036-0.038, Ni 0.078-0.084, Si 0.30-0.32, Mo 0.030-0.034, Cu 0.18-0.21.

The static mechanical properties of the base metal: upper yield stress $R_{eH} = 282 - 288$ MPa, lower yield stress $R_{eL} = 268 - 277$ MPa, ultimate strength $R_m = 428$ MPa, elasticity module $E = 213$ GPa, elongation $A = 38$ %, reduction in area $Z = 72$ %, and the weld metal: $R_{eH} = 385$ MPa, $R_{eL} = 370$ MPa, $R_m = 475$ MPa, $E = 211$ GPa, $A = 34$ %, $Z = 78$ %. The hardness of basic metal is BHN = 126-131. The seam's metal is harder: BHN = 147-159.

Microstructure of welded plate is presented in Fig. 1., a – ferite and dark pearlite grains; b – non-homogeneous microstructure with common for welds the ferite, pearlite, austenite strips and dendritic structures; c – in the HAZ there are the ferite, pearlite and carbide phases.

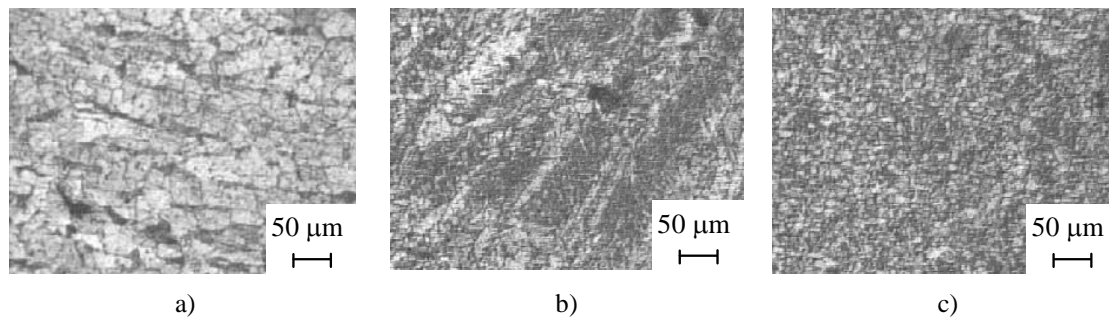


Figure 1. The structure of the plate: a) basic metal; b) weld metal; c) heat affected zone

To determine the coefficient of the limit stress rate (cracking threshold) ΔK_{th} , compact specimens under eccentric tension (CT) with a cut were made (see Fig 2a). The base metal and welded joint specimens, with the cyclic frequency of 20 ... 30 Hz, were tested. The fracture of the specimen is shown in Fig 2b.

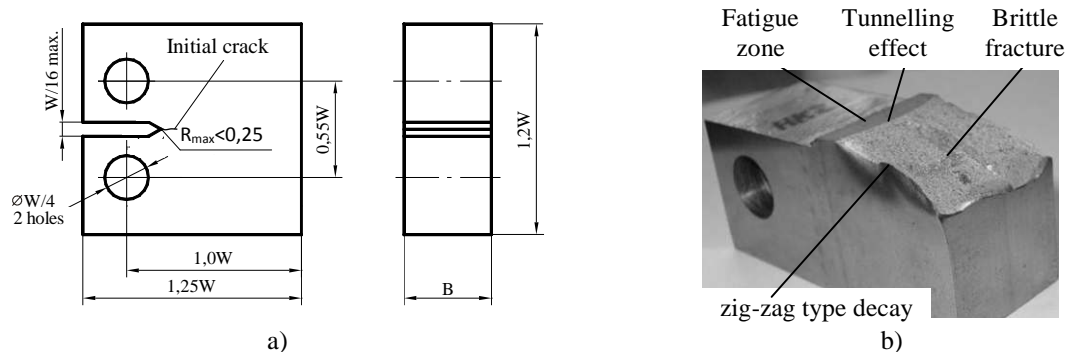


Figure 2. CT specimen: a) scheme; b) fracture after test

The stress intensity factor is calculated by the formula ASTM E 647-00:

$$K = (F/W^{1/2}) \cdot f(\lambda), \quad (2.1)$$

where $f(\lambda) = \left[\frac{2 + \lambda}{(1 - \lambda)^{3/2}} \right] \cdot (0,866 + 4,64\lambda - 13,32\lambda^2 + 14,72\lambda^3 - 5,6\lambda^4)$, $\lambda = a/W$, F – tensile force, B – specimen's thickness, W – specimen's basis, a – crack size.

The interval of the stress intensity factor is $\Delta K = K_{max} - K_{min}$; the coefficient of stress cycle asymmetry is $r = F_{min} / F_{max} = K_{min} / K_{max}$; K_{min} and K_{max} are the smallest and the largest values of the stress intensity factor per loading cycle.

Nominal stresses on the tip of the crack are calculated by the formula:

$$\sigma = \frac{2F}{B \cdot W} \cdot \frac{2 + \lambda}{(1 - \lambda)^2} \quad (2.2)$$

The testing was performed according to the specified methods, when the cycle asymmetry coefficient was $r \approx 0$. To apply the experimental data to actual calculation, the variation of stress cycle asymmetry should be taken into account.

The relationship between the cracking thresholds for different cycle asymmetry coefficients is as follows:

$$\Delta K_{th} = \Delta K_{th0} (1 - r)^\gamma, \quad (2.3)$$

where ΔK_{th} is stress intensity factor of cracking threshold; ΔK_{th0} is stress intensity factor of cracking threshold, when $r = 0$; γ is the indicator of the material properties, ranging from 0,5 to 1.

The testing of CT specimens allowed the authors to determine the values of the cracking threshold ΔK_{th} and the relationships between the rate of crack propagation and the interval of the stress intensity factor (see Fig 3). The limiting stress intensity factor ΔK_{th} (it is assumed that $\Delta K = K_{max}$) is determined, when the cycle asymmetry coefficient $r \approx 0.05$.

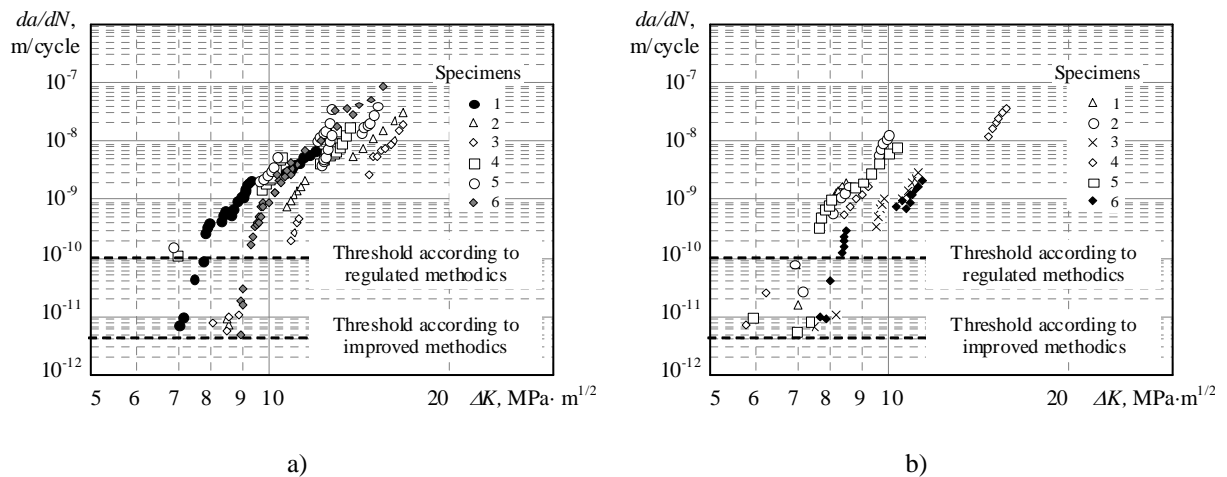
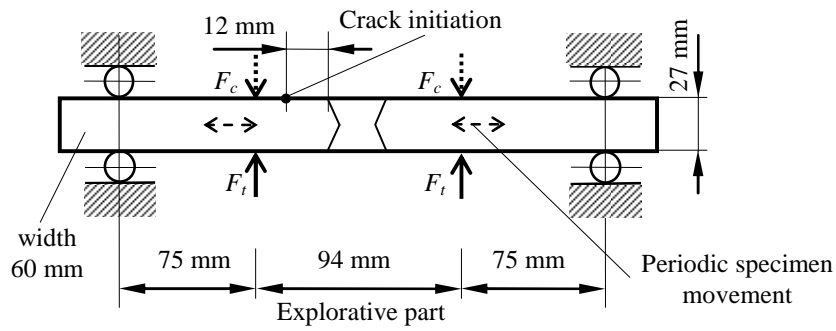
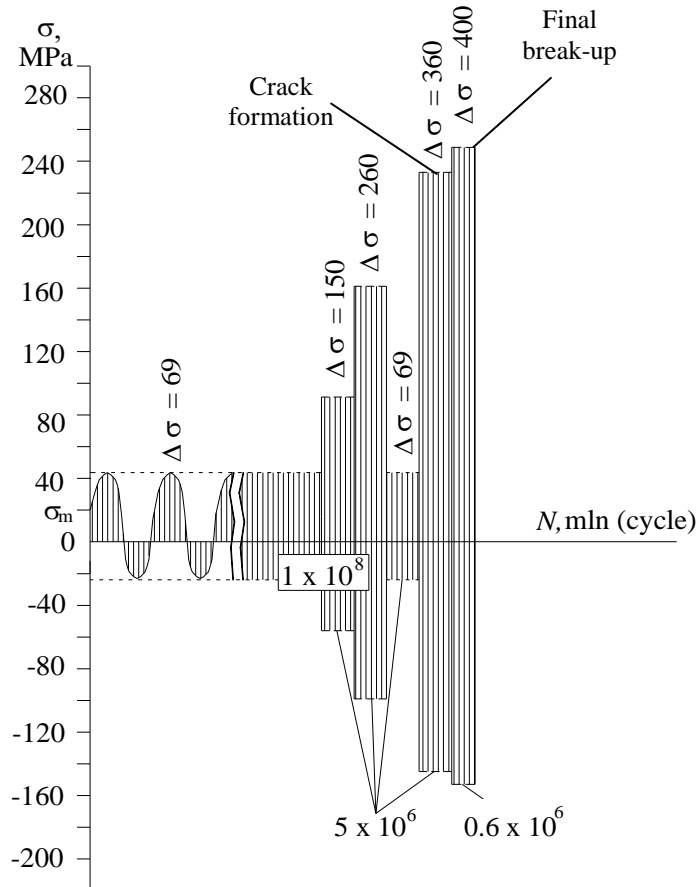


Figure 3. Crack growth rate versus the range of stress intensity factor in CT specimens: a) of basic metal; b) of the weld (crack is along or near the weld)

In Fig 4, the loading history (at the frequency of 20 Hz) of a semi-natural specimen is presented. The loading is chosen according to the operation conditions of mining equipment. The initial loading $\Delta\sigma = 69$ MPa ($\sigma_{max} = 42.8$ MPa, $\sigma_{min} = -26.2$ MPa, $r = -0.62$) corresponds to the actual loading of the rotating mineral mill drums and supports, taking into account the safety factor. The specimen was tested during $1 \cdot 10^8$ loading cycles, with periodical breaks for crack formation inspection by non-destructive methods. Then, the loading stages, when $\Delta\sigma = 150$ MPa, $\Delta\sigma = 260$ MPa and $\Delta\sigma = 69$ MPa again, followed. When the stress interval reached $\Delta\sigma = 360$ MPa, some flaws could be detected on the surface under maximal stress in the vicinity of the weld and on the plate. Further loading led to crack propagation on the plate surface, but not around the weld. When stresses reached $\Delta\sigma = 400$ MPa, crack propagation on the surface and deeper could be observed on one side of the plate. When the critical size of the crack was reached, the fracture of the specimen could be observed.



a)



b)

Figure 4. Semi-natural specimen loading scheme (a) and loading program (b)

In Fig 5, the investigated part before and after testing is shown. One can see that crack propagation and complete failure of the specimen take place at the distance of 12 mm from the edge of the weld. In Fig 6, the view of the fracture of the specimen, demonstrating the crack origin, is presented. The analysis of the fracture, using SEM, allowed the authors to determine the cause of crack formation (see Fig 7). The fractographic analysis of some damaged areas has shown the presence of various heterogeneous formations (see Figs 8,9). Their spectral analysis is presented in Tables 1,2. These are the inclusions of manganese sulphate (dark) and cementite (light) of various forms and sizes. One of them became the centre of crack formation on the plate surface. The resistance of the specimens to high-cycle loading ($N > 10^8$) has some specific features.

Considering crack propagation, one should take into account that the action of various fracture mechanisms can be observed at various stages of crack formation (i.e. crack initiation, its stable growth and the complete failure of the element). Comprehension of the fracture mechanism of the

material and quantitative evaluation of fracture parameters allows us to improve the methods of calculating the cyclic strength of structures and more accurately determine their longevity. This also helps to improve building materials and technological processes of their production. The fatigue fracture mechanism is associated with several stages, characteristic of most metal structures. They include the initiation and propagation of small cracks, the initiation and propagation of short cracks, and propagation of the fatigue cracks until the complete failure of the element occurs.

The mechanism of small cracks' origination is based on the accumulation of dislocations, causing the increase of local stresses. Due to cycle stresses, the dislocations emerge and propagate on the planes, where the tangential stresses are the highest.

Geometric and microstructural heterogeneities (e.g. inclusions, voids, grain boundaries, traces of carbide and other undesirable chemical compounds) do not strongly affect long cracks, but may strongly affect the rate and direction of short cracks' growth due to their similar size.

When the fatigue fracture takes place, a long crack grows at the expense of small cracks, emerging on its tip, which merge to make a small crack of the critical size. The latter, in turn, merges with the main crack.

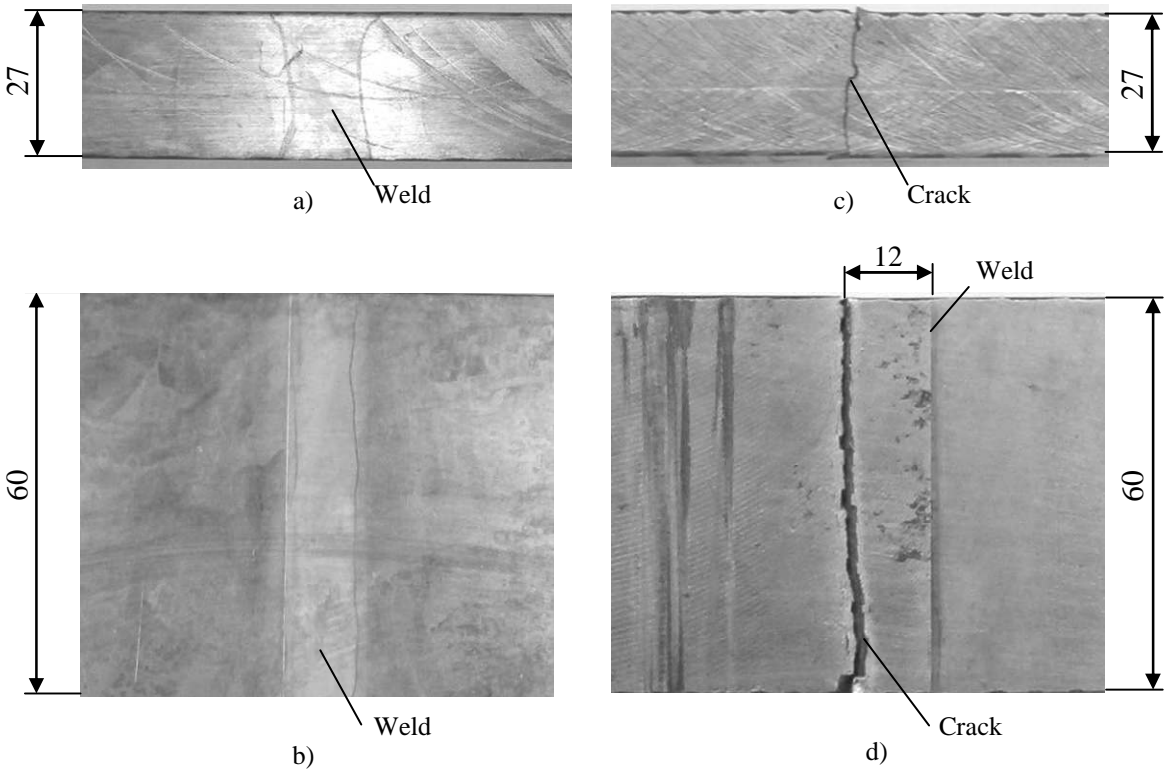


Figure 5. View of the tested section before and after testing: a, b – seam locale; c, d – fracture locale

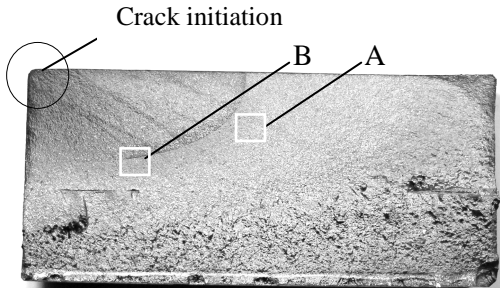


Figure 6. Fracture of the specimen

The experimental investigation of a semi-natural specimen has shown that cracks may be formed not only in the vicinity of the weld of the welded plates. If there are some casting defects in the plate material, they may become the centres of cracks. This happens in spite of various defects in the heat affected area, emerging in the process of welding. The performed experimental study has shown that the technology of welding the investigated plates is rather high and their inspection by non-destructive methods has not revealed any defects.

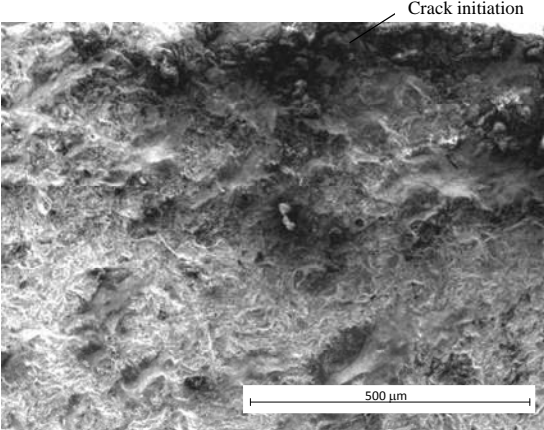


Figure 7. Crack initiation zone

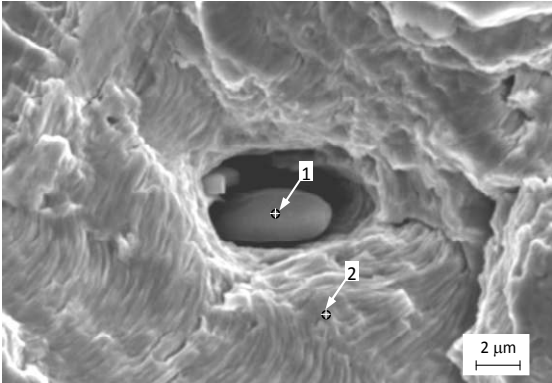


Figure 8. Fracture fragment A according Fig. 6

Table 1. Chemical composition in different points, %

Points	C	O	S	Mn	Fe
1	1.45	2.89	27.14	53.85	14.67
2	3.22	0.40	0.11	0.32	95.95

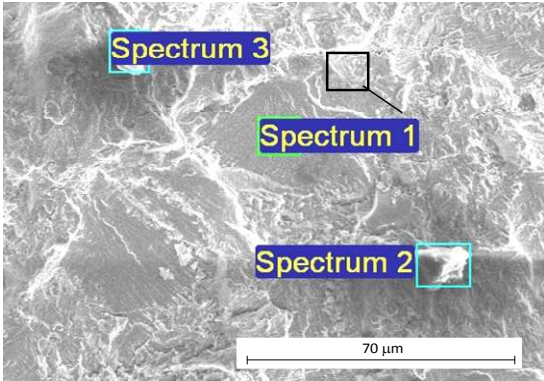


Figure 9. Fracture fragment B according Fig. 6

Table 2. Chemical composition in different points, %

Points	C	O	S	Mn	Fe
1	7.22	8.48	0.18	0.88	83.24
2	47.97	14.38	0.88	0.57	36.20
3	48.31	12.63	0.41	0.43	38.21

The evaluation of the homogeneity of materials and cracks in engineering calculations is a complicated problem, therefore, a higher safety factor and a larger mass of a structural element should be used. Applying the principles of fracture mechanics to calculating the cycle strength of structural elements, the efforts are made to determine the critical stress value, at which the crack would not propagate, or to find the critical crack size, given the stresses acting in a structural element.

The calculation of the essential structural elements of mining power generating and chemical equipment is performed, applying the assumption about the prevention of the fatigue crack emergence. Various methodologies (Žiliukas, 2011, Anderson, 2005; Makhutov, 2005 and the others) are based on various criteria of fracture, including stress intensity factor K , the J-integral, the limit crack opening δ , etc. The admissible (design) stresses are related to the safe crack size as follows:

$$[\{K_I, J, \delta\}] = \left\{ \frac{\sigma_{th}}{n_\sigma}, l_{adm}, n, \dots \right\} \geq \frac{\{K_{th}, J_{cth}, \delta_{cth}\}}{n_{\{K_I, J, \delta\}}}, \quad (2.4)$$

where $[\{K_I, J, \delta\}]$ and $\{K_{th}, J_{cth}, \delta_{cth}\}$ are the admissible and limiting parameters of fracture mechanics. The safety factor $n_{\{K_I, J, \delta\}}$ shows how many times the parameter of fracture mechanics $\{K_I, J, \delta\}$ should be reduced because of the increase of the crack length under the admissible (design) stresses that they could reach the critical values $\{K_{th}, J_{cth}, \delta_{cth}\}$. Given $n_{\{K_I, J, \delta\}} = 1$, the critical crack length l_{cr} , corresponding to the admissible stresses, is obtained and, given $n_{\{K_I, J, \delta\}} > 1$, the admissible crack size $l_{adm} < l_{cr}$ is obtained. The accurate values of the safety factor may be calculated by using various critical parameters. The safe state is guaranteed by using the limit safety factor $n_{\{K_I, J, \delta\}}$, which decreases the value of fracture mechanics criterion (resistance to cracking). In this way, the critical crack size l_{cr} is also decreased to the admissible value l_{adm} under the variable design stresses $\Delta\sigma$:

$$\Delta\sigma \leq \Delta\sigma_{th adm} = \frac{\Delta\sigma_{th}}{n_\sigma}, \quad (2.5)$$

where $\Delta\sigma_{th adm}$ denotes the admissible cycle stresses; $\Delta\sigma_{th}$ is the limit of cyclic strength; n_σ is the safety factor according to the cyclic strength limit.

This methodology is used for calculating the cyclic strength of basic structures. It is considered that fatigue cracks do not develop, when the condition given below is satisfied:

$$\Delta K_I \leq [K_I] = \frac{\Delta K_{th}}{n_K}, \quad (2.6)$$

The limiting stress intensity factor range obtained after CT specimens testing was $\Delta K_{th} = 7,0 \dots 9,0$ MPa \sqrt{m} at crack propagation rate 10^{-11} m/cycle. This corresponds to the maximum limiting stresses $\Delta\sigma_{th} = 65 \dots 90$ MPa. In comparison with operational maximum stress $\Delta\sigma_{max} = 42,8$ MPa the safety factor is $n_\sigma \approx 2$. By increasing of the stresses of semi-natural specimen program loading up to $\Delta\sigma = 150$ MPa ($\sigma_{max} = 93$ MPa) the safety factor comes to $n_\sigma \approx 1$.

Based on the performed experimental and analytical research, the safety margin of the cyclic strength of structures may be evaluated by calculating the stress intensity factor (under various loads) or by

comparing the cracking threshold stresses of CT specimens to the stresses, developing in the elements of real structures. The testing of a semi-natural specimen according to program loading has shown the structural element's behaviour under overloading conditions (including seismic loads). Cyclic strength calculations can be performed according to submitted references list or by the use of the other relevant sources.

CONCLUSIONS

1. The performed research allowed the authors to determine the main principles of crack initiation and propagation in welded steel specimens under cyclic loading.
2. The limits of the rate of crack propagation and the interval of the limiting stress intensity factor were determined for CT specimens with cracks, propagating in the base metal ($\Delta K_{th} = 7-9 \text{ MPa}\cdot\text{m}^{1/2}$, when crack growth rate $v = 10^{-11} \text{ m/cycle}$) and in the weld ($\Delta K_{th} = 6-8 \text{ MPa}\cdot\text{m}^{1/2}$, when crack growth rate $v = 10^{-11} \text{ m/cycle}$).
3. During the experimental investigation of a semi-natural specimen, crack origins were not registered under stresses, approaching operational stresses. The crack origin was registered at $\Delta\sigma = 360 \text{ MPa}$ in the area of maximal stresses, which developed at the distance of 12 mm from the weld edge.
4. Fractographic analysis revealed the cause of crack development in the semi-natural specimen, which was the inhomogeneous formation, strongly affecting the crack growth rate and direction.

REFERENCES

- Anderson, T.L. (2005). Fracture Mechanisms, Taylor & Francis, CRC Press.
- ASTM E 1681-95. (1995). Standard Test Method for Determining a Threshold Stress Intensity Factor for Environment-Assisted Cracking of Metallic Materials Under Constant Load.
- ASTM E 647-00. (2002). Standard Test Method for Measurement of Fatigue Crack Growth Rates.
- Bražėnas, A. 2002. Strength and Low Cycle Fatigue of Mechanically Heterogeneous Butt Welded Joints, Monograph, Technologija, Kaunas.
- Billaudeau, T. and Nadot, Y. (2004). Support for an environmental effect on fatigue mechanisms in the long life regime, *Int. J. of Fatigue* **26:8**, 839-847.
- Makhtov, N.A. (2005). Structural strength, resource and technogenic safety, vol.1, vol.2, Nauka, Novosibirsk.
- Radaj, D., Sonsino, C.M. and Fricke, W. (2006). Fatigue Assessment of Welded Joints by Local Approaches, Woodhead Publishing Limited and CRC Press LLC.
- Ravi, S., Balasubramanian, V. and Nemat Nasser, S. (2004). Effect of Notch Location on Fatigue Life Prediction of Strength Mismatched HSLA Steel Weldments. *J. Mater* **20:2**, 129-135.
- Schijve, J. (2009). Fatigue of Structures and Materials, Springer Science, Business Media, B.V.
- Stychev, S. and Kujawski, D. (2005). Analysis of crack propagation using ΔK and K_{max} . *Int. J. Fatigue* **27**, 1425-1431.
- Stonkus, R., Leonavičius, M. and Krenevičius, A. (2009). Cracking threshold of the welded joints subjected to high-cyclic loading, *Mechanika* **2:76**, 5-10.
- Stonkus, R. and Leonavičius, M. (2010). The high cyclic failure analysis of welded joints of CT specimens // Solid State Phenomena Vol. 165 Mechatronic Systems and Materials: Materials Production Technologies. pp 183-188, Trans Tech Publications, Switzerland.
- Wang, P.C. (1995). Fracture mechanics parameter for the fatigue resistance of laser welds. *Int. of Fatigue*, **1:17**, 25-34.
- Žiliukas, A. (2012). Strength and failure criteria, EMAS Publications.